Supporting Information

A ratiometric electrochemical biosensor for glycated albumin detection based on enhanced nanozyme catalysis of cuprous oxide-modified reduced graphene oxide nanocomposites

Zhi Li [a], Jingwen Zhang [a], Ge Dai [a], Feifei Luo [a], Zhaohui Chu [a], Xing Geng [a], Pingang He [a], Fan Zhang [a], Qingjiang Wang [a,*]

[a] *School of Chemistry and Molecular Engineering, East China Normal University, 500 Dongchuan Road, Shanghai 200241, PR China*

* Corresponding author. Tel: +86 21 54340015

E-mail: qjwang@chem.ecnu.edu.cn

Contents

1. Experimental section

1.1 Apparatus

X-ray photoelectron spectroscopy (XPS) was conducted on a Kratos Axis UltraDLD photoelectron spectroscope (AXIS UltraDLD, Japan). Scanning electron microscopy (SEM) and SEM-EDS were measured by a Hitachi S-4800 scanning electron microscope (Hitachi S-4800, Japan). Transmission electron micrograph (TEM) was obtained on a JEM-2100 transmission electron microscope (JEOL, Japan) operating at an accelerating voltage of 200 kV. Atomic force microscope (AFM) images were recorded using tapping mode AFM (Multimode 8, Bruker). The electrochemical experiments were carried out with a CHI660E electrocheimical workstation (CHI 660E, Shanghai CH Instruments, China) with a conventional three-electrode system consisting of a glassy carbon electrode (GCE), saturated calomel electrode (SCE) and platinum wire as working, reference and counter electrodes, respectively. UV-Vis spectra were performed with a cary 50 probe UV-Vis spectrophotometer (Varian, USA). The GA ELSIA kit were analyzed using the Biotek Synergy Neo2 fluorescent microplate reader (Biotek, Winooski, Vermont, USA).

1.2 Electrocatalytic experiments

The glassy carbon electrode (GCE, φ = 3 mm) was initially polished with 1.0 and 0.05 μm alumina slurry. The electrode was afterwards sonicated in the ethanol and deionized water for 5 min, separately, to remove the excess Al_2O_3 powder. The Cu_2O-rGO NCs were dispersed in the mixture of ethanol and deionized water (V/V = 1:2) under sonicating to obtain black suspension with a concentration of 1 mg·mL^{-1}. 5 μL Cu_2O-rGO NCs (1 mg·mL^{-1}) was dropped on the prepared GCE and dried in air. Then, Cu_2O-rGO/GCE was immersed in a MB-tDNA solution (250 nM) at 4 °C overnight. The MB-tDNA/Cu_2O-rGO/GCE was immersed in various concentration of the GA solution and incubated for 50 min.

The measurements of cyclic voltammetry (CV) and differential pulse voltammetry (DPV) were performed on the electrochemical workstation. CV detection buffer, 10 mM PBS containing 5 mM $Fe(CN)_6^{3-/4-}$ (1:1) and 0.1 M KCl (pH 7.4). DPV detection buffer, 10 mM PBS containing 0.1 M NaOH and 1 mM glucose. Electrode washing buffer, 10 mM Tris-HCl containing 50 mM KCl (pH 7.4). The parameters of CV are as follows: potential range, -0.6 V to +0.8 V; scan rate, 0.05 V/s. The parameters of DPV are as follows: potential range, -0.6 V to +0.8 V; pulse width, 0.05 s; sample width, 0.0167 s; pulse period, 0.2 s; quiet time, 2 s.

1.3 Serum sample preparation

These serum samples were derived from normal (C57BL/6) or diabetic mice (B6.BKS(D)-$Lepr^{db}$/J). The mice (18-22 g) were purchased from Shanghai Biomodel Organism Science & Technology Development Co., Ltd (Shanghai, China). The age at the time of recording was 2-3 months. Serum samples were obtained by centrifugation clotted blood at 4000 rpm for 10 min, and then collected and stored at 4 °C for further use.

All procedures involving animals were conducted with approval of the Animal Ethics Committee in East China Normal University (the license number: m20190303). The information of guidelines are as follows: This animal experiment method and purpose conform to human moral and ethical standards and international practice, and compliance with relevant regulations, principles of ethical welfare of experimental animals and rules and regulations of experimental animal center during animal experiments.

2. Characterization of Cu_2O-rGO NCs

2.1 EDX mapping images

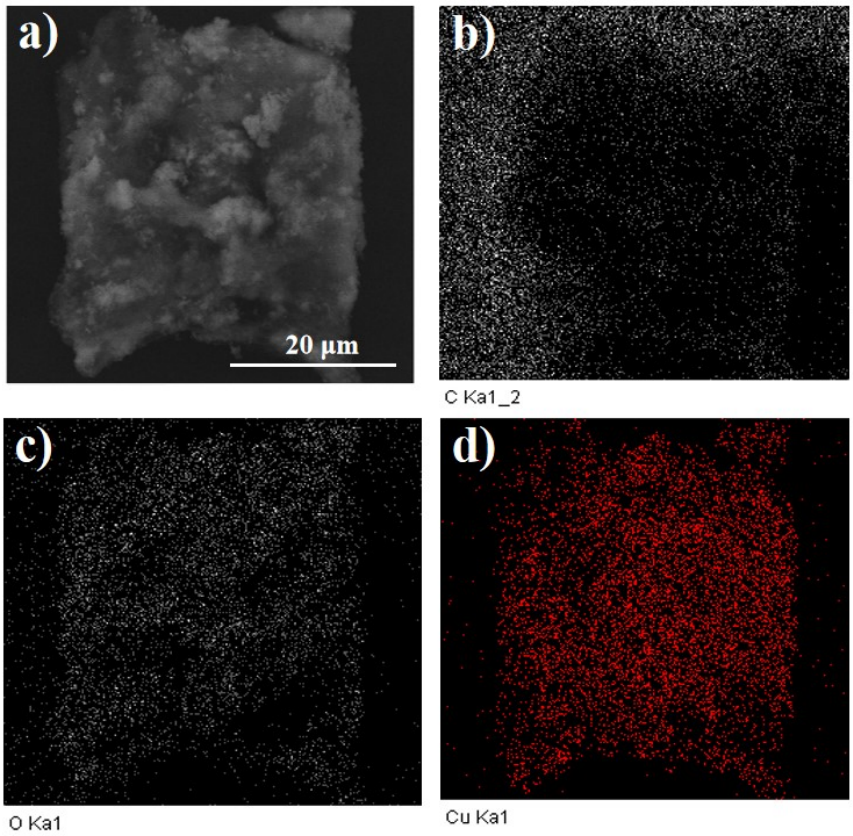

Figure S1. (a) SEM images of Cu_2O-rGO NCs; elemental mapping of C (b), O (c) and Cu (d).

2.2 XPS characterization

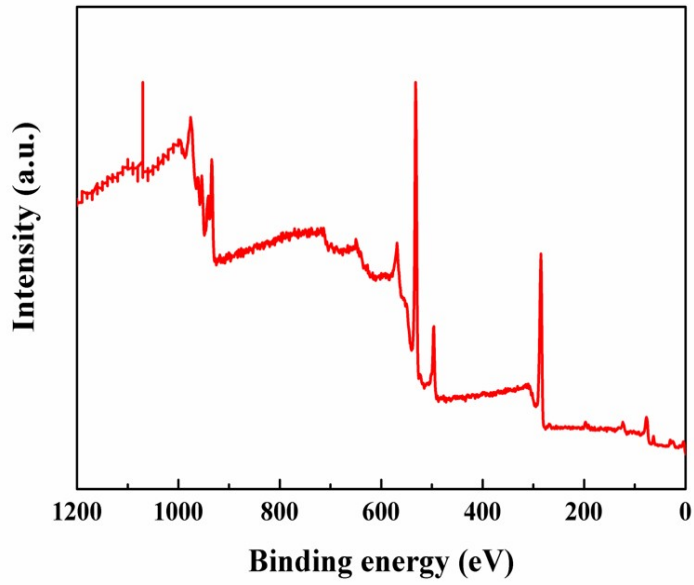

Figure S2. XPS survey scan spectrum of the Cu_2O-rGO NCs.

2.3 TEM characterization

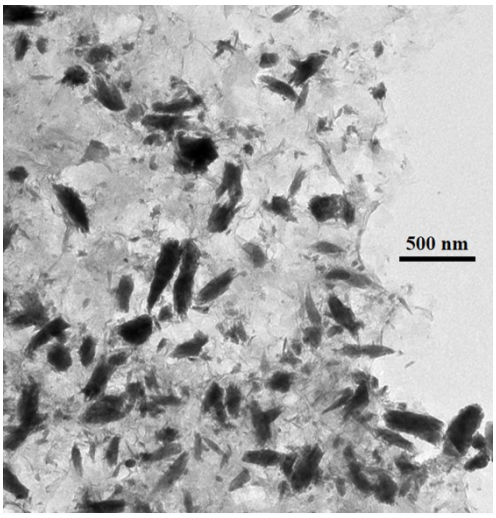

Figure S3. TEM image of the Cu_2O-rGO modified substrate.

2.4 The effective area of Cu_2O-rGO/GCE

The effective area of the Cu_2O-rGO/GCE can be calculated from electrochemical measurements via the Randle-Sevcik equation (1).

$$i_p = 2.69 \times 10^5 A C_0 n^{3/2} D_R^{1/2} v^{1/2} \quad (1)$$

Table S1. Electrochemical parameters at different scan rates of the modified electrode by CV measurements.

System	Scan rate (V/s)	E_{pc} (V)	E_{pa} (V)	ΔE_p (V)	i_{pc} (μA)	i_{pa} (μA)	i_{pc}/i_{pa}
5 mM $Fe(CN)_6^{3-/4-}$ (1:1)	0.02	0.253	0.140	0.113	74.89	-72.82	-1.028
	0.05	0.262	0.130	0.132	112.7	-106.9	-1.054
	0.1	0.274	0.117	0.157	150.0	-140.0	-1.071
	0.2	0.295	0.101	0.194	186.5	-168.6	-1.106

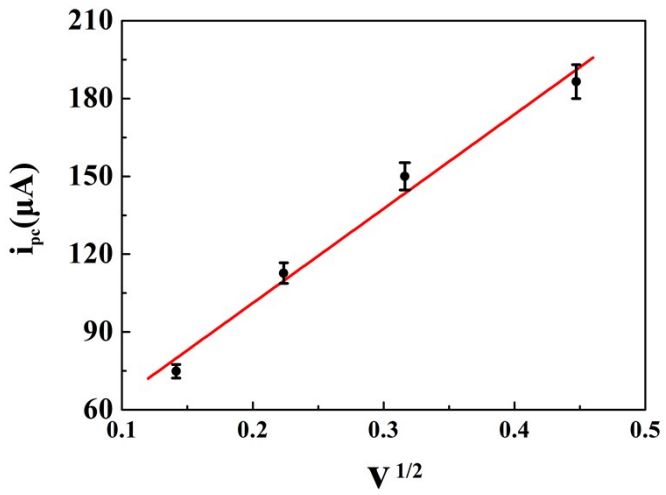

Figure S4. The linear equation of between the i_{pc} and $v^{\frac{1}{2}}$.

In this strategy, the effective area has been obtained by CV measurements. A linear equation is established between the value of the i_{pc} (μA) and $v^{\frac{1}{2}}$. The slope of the linear equation is 363.68. The effective area of the Cu_2O-rGO/GCE based on the Randle-Sevcik equation is 0.0855 cm^2. The effective area is higher than the geometric area (0.0707 cm^2). The result provides the Cu_2O-rGO NCs have the 3D interconnected porous architecture the surfaces and these Cu_2O-rGO NCs are very rough, the defects can serve as both highly active catalytic sites and electron reservoirs.

3. Mimetic catalytic activity of Cu_2O-rGO NCs

3.1 UV-vis behaviors of Cu_2O-rGO NCs towards TMB

The effect of nanozyme amount was screened on Cu_2O-rGO NCs from 1 to 20 μg·mL^{-1} under the same conditions. The reaction was performed by using 1-20 μg·mL^{-1} of Cu_2O-rGO NCs, TMB solution (8.32 mM, 20 μL) and H_2O_2 (100 mM, 100 μL) in sodium acetate buffer (total volume is 1 mL). The time-dependent change of UV-Vis absorbance at 652 nm was recorded over 10 min at room temperature.

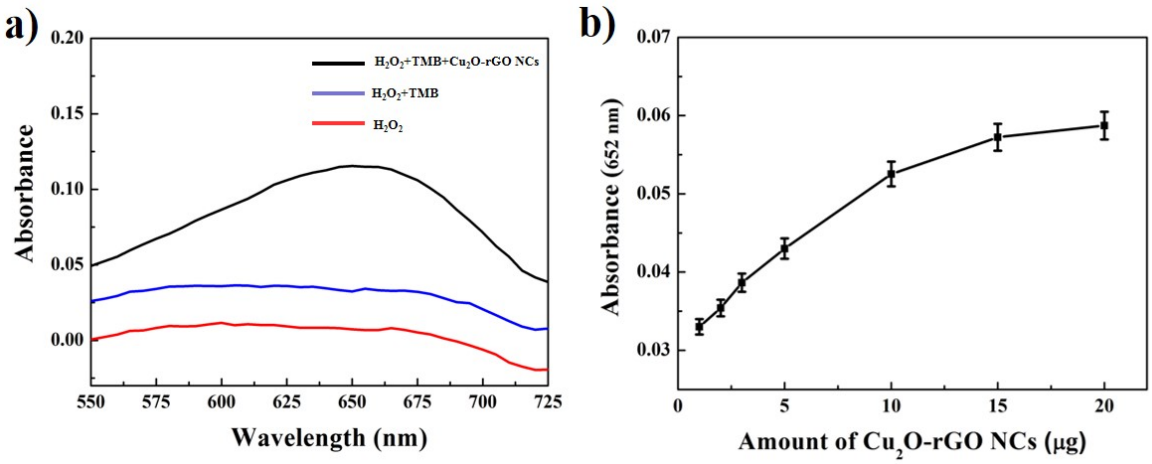

Figure S5. Typical absorption spectra of TMB-H_2O_2 solution in the absence and presence of Cu_2O-rGO NCs: H_2O_2, H_2O_2+TMB, and H_2O_2+TMB+Cu_2O-rGO NCs (a); Mass effect of the added Cu_2O-rGO NCs in the system from 1 to 20 μg (b).

3.2 The steady-kinetic analysis based on Michaelis-Menten model

The Michaelis-Menten constant K_m and maximum reaction velocity V_{max} were calculated according to the Michaelis-Menten equation (2):

$$\frac{1}{V} = \frac{K_m}{V_{max}} \bullet \frac{1}{[S]} + \frac{1}{V_{max}} \quad (2)$$

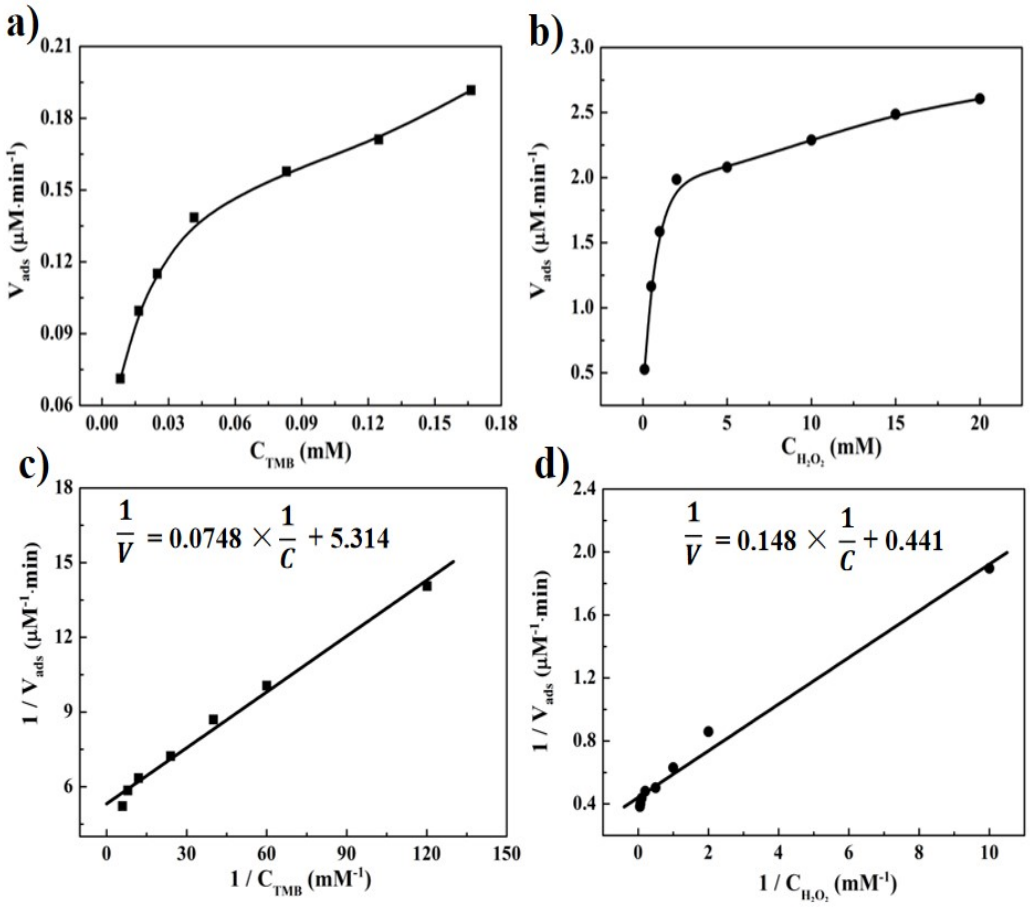

Figure S6. The stead-state kinetic analysis based on Michaelis-Menten model (a and b); Lineweaver-Burk double-reciprocal model (c and d). The concentration of H_2O_2 was fixed at 10 mM while TMB concentration was varied from 0.00832 mM to 0.1664 mM; The concentration of TMB was fixed at 0.1664 mM and H_2O_2 concentration was altered from 0.1 mM to 20 mM.

Table S2. Comparison of the apparent Michaelis-Menten constant (K_m) and the maximum reaction rate (V_{max}) calculated from the Lineweaver-Burk double reciprocal plots.

Catalyst	Substrate	K_m (mM)	V_{max} (μM·min^{-1})	Ref.
2.6Pt/EMT	TMB	0.16	2.83	S1
	H_2O_2	0.58	6.96	
HRP	TMB	0.43	6	S2
	H_2O_2	3.73	5.23	
Cu@Cu_2O aerogels	TMB	0.94	5.71	S3

3NiV-400	TMB	0.437	1.884	S4
	H_2O_2	15	1.212	
GDYO	TMB	0.62	1.15	S5
	H_2O_2	2.59	1.06	
Cu_2O-rGO NCs	TMB	0.014	0.19	This work
	H_2O_2	0.34	2.27	

4. The effect of pH value for GA sensor

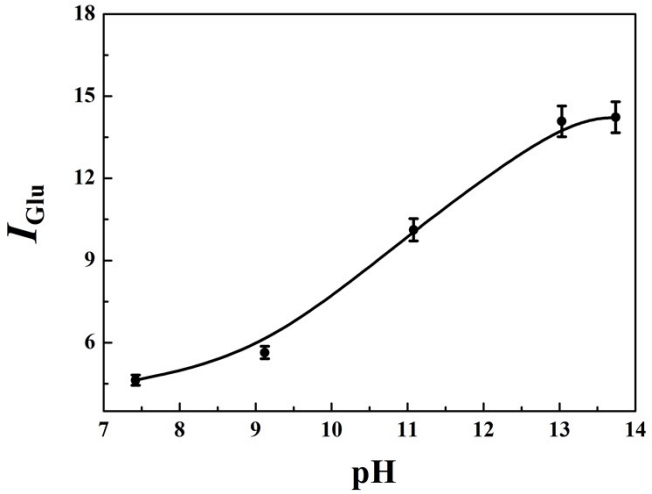

Figure S7. Striping peak currents of the glucose oxidation (I_{Glu}) versus the pH value (7.42, 9.12, 11.08, 13.03 and 13.74) of the DPV detection buffer.

5. The repeatability, reproducibility and stability of the GA sensor

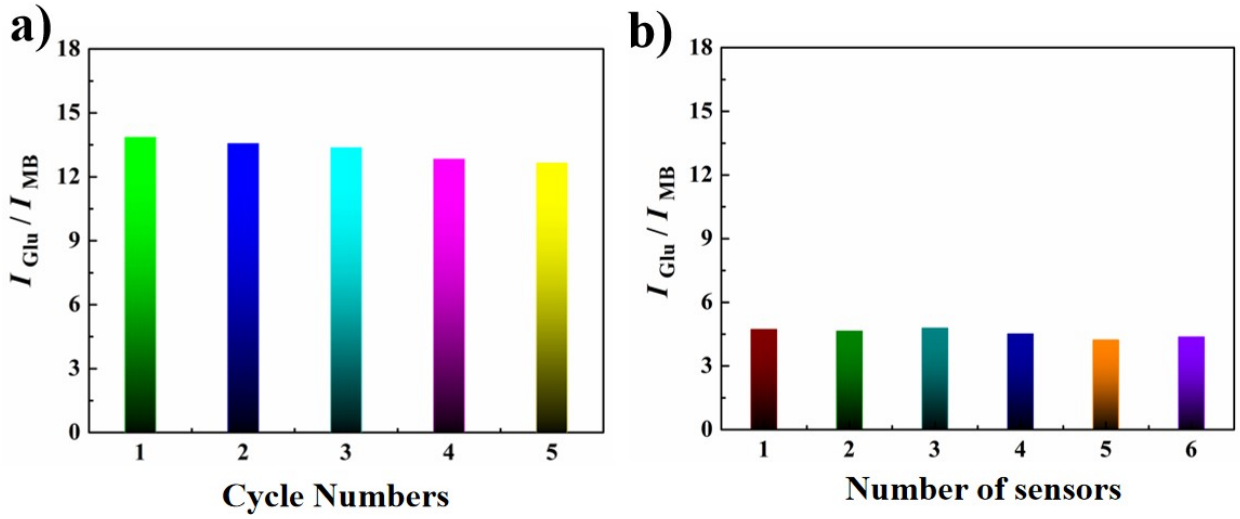

Figure S8. (a) DPVs of the electrochemical ratiometric sensor under containing scanning for 5 cycles in 10 mL of 10 mM PBS containing 0.1 M NaOH and 1 mM glucose. (b) The reproducibility of 6 biosensors towards GA of 2 $\mu g \cdot mL^{-1}$.

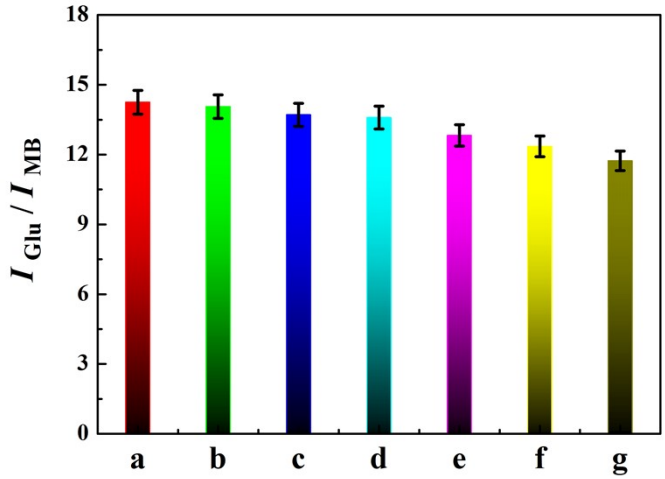

Figure S9. Stability of the ratiometric sensor via DPV for 1 day (a), 2 days (b), 3 days (c), 4 days (d), 5 days (e), 6 days (f) and 7 days (g).

References

S1. Li, X.; Yang, X.; Cheng, X.; Zhao, Y.; Luo, W.; Elzatahry, A. A.; Alghamdi, A.; He, X.; Su, J.; Deng, Y. Highly dispersed Pt nanoparticles on ultrasmall EMT zeolite: A peroxidase-mimic nanoenzyme for detection of H_2O_2 or glucose. *J. Colloid. Interf. Sci*., 2020, **570**, 300-311.

S2. Yang, X.; Qiu, P.; Yang, J.; Fan, Y.; Wang, L.; Jiang, W.; Cheng, X.; Deng, Y.; Luo, W. Mesoporous materials-based electrochemical biosensors from enzymatic to nonenzymatic. *Small*, 2021, **17**, 1904022.

S3. Ling, P.; Zhang, Q.; Cao, T.; Gao, F. Versatile three-dimensional porous Cu@Cu_2O aerogel networks as electrocatalysts and mimicking peroxidases. *Angew. Chem. Int. Ed*., 2018, **57**, 6819-6824.

S4. Chen, C.; Wang, Y.; Yang, Z.; Zhang, D. Layered double hydroxide derived ultrathin 2D Ni-V mixed metal oxide as a robust peroxidase mimic. *Chem. Eng. J*., 2019, **369**, 161-169.

S5. Ma, W.; Xue, Y.; Guo, S.; Jiang, Y.; Wu, F.; Yu, P.; Mao, L. Graphdiyne oxide: a new carbon nanozyme. *Chem. Commun*., 2020, **56**, 5115-5118.